

A quantum Otto engine with finite heat baths: energy, correlations, and degradation

Alejandro Pozas-Kerstjens,¹ Karen V. Hovhannisyanyan,^{1,2} and Eric G. Brown¹

¹*ICFO-Institut de Ciències Fòniques, The Barcelona Institute of Science and Technology, 08860 Castelldefels (Barcelona), Spain*

²*Department of Physics and Astronomy, Ny Munkegade 120, Aarhus University, DK-8000 Aarhus, Denmark*

We study a driven harmonic oscillator operating an Otto cycle between two thermal baths of finite size. By making extensive use of the tools of Gaussian quantum mechanics, we directly simulate the dynamics of the engine as a whole, without the need to make any approximations. This allows us to understand the non-equilibrium thermodynamics of the engine not only from the perspective of the working medium, but also as it is seen from the thermal baths' standpoint. For sufficiently large baths, our engine is capable of running a number of ideal cycles, delivering finite power while operating with maximal efficiency. Thereafter, having traversed the baths, the perturbations created by the interaction start deteriorating the engine's performance. We additionally study the correlations generated in the system, and relate the buildup of working medium-baths and bath-bath correlations to the degrading performance of the engine over the course of many cycles.

I. INTRODUCTION

The second law of thermodynamics prohibits extracting mechanical work from systems in thermal equilibrium. Therefore, in order to obtain work, one has to have access to systems out of thermal equilibrium. The theoretically simplest out-of-equilibrium system is one composed by two subsystems that are each at individual equilibrium and at different temperatures. This is the traditional setup for a heat engine: a working medium (WM) reciprocating between two thermal baths, pumps heat from the hotter bath (at temperature T_h) to the colder one (at temperature T_c) and outputs work as a result. The ideal engine converts the internal energy of the hot bath into work with an efficiency given by Carnot's formula, $\eta_C = 1 - T_c/T_h$. The idealizations needed for the machine to operate at such an efficiency are that (i) the baths interact with the working medium weakly [1, 2], (ii) the cycle is a quasiequilibrium process and hence it takes infinite time to complete [1, 3, 4], and (iii) the baths are infinitely large [1, 5–8]. It has to be noted, however, that the size of the working medium itself is of no relevance – it can be anything from a two-level quantum system [9–11] to a giant steam engine [12].

Strictly speaking, conditions (i) and (ii) can never be satisfied: any interaction has finite strength and any process that can be observed takes finite time. In the generic setup where the bath is a many-body system with short-range interactions and the WM couples to it locally, the breakdown of (ii) entails the failure of (iii) even if the bath is infinitely large [13]. Indeed, in such systems the Lieb-Robinson bounds [14, 15] imply that, roughly speaking, the correlations spread with finite velocity. This means that, in finite time, the WM can have access to only a finite region of the bath (see [16] where this idea was brought to use for the first time). However, it should be emphasized that the said finite region gets re-thermalized by the rest of the bath, so this scenario is not entirely equivalent to a finite bath.

Despite the significant attention that finite-time [3, 4,

17–27], strong-coupling [27–36], and finite-size [5, 7, 8, 16, 37–39] effects have been getting either one by one or in groups of two, a rigorous microscopic analysis of a finite-power thermal machine strongly coupled to finite-size heat baths has never been carried out. In this work, we aim to fill this gap by performing a fully microscopic analysis of a heat engine consisting of a harmonic oscillator serving as WM, reciprocating—by being alternately strongly coupled and decoupled—between two finite, initially thermal harmonic chains serving as thermal baths.

The WM interacts with the baths via a modulated linear coupling (see Sec. III for details). This type of system-reservoir interaction is known under the name of Caldeira-Leggett model [40], and is routinely used in many areas of physics ranging from quantum Brownian motion to quantum optics [41, 42].

The engine runs a strong-coupling adaptation of the Otto cycle [12]: the two “isochoric” thermalizations are intermediated by two “adiabatic” quenches of the WM's frequency (see Sec. IV for the precise description). For the first cycle, the WM starts uncoupled from the baths and at equilibrium with the cold bath. This makes the initial state of the overall system a Gaussian state. Given that the total Hamiltonian is quadratic at any moment of time, the dynamics of the system can be described within the formalism of Gaussian quantum mechanics (GQM) [43]. The latter maps the intractable Schrödinger equation in the infinite-dimensional Hilbert space of the overall system onto a linear evolution of the finite-dimensional phase space. This allows us to perform a comprehensive analysis of the machine's operation without the need to adhere to any of the many approximations usually made when dealing with quantum open-system dynamics [41, 42]. Moreover, by directly simulating the overall system's evolution, we gain access to the states of the baths at any moment of time, which allows us to reveal the physical mechanisms governing the degradation and eventual exhaustion of the initial disequilibrium provided by the baths in the finite-size, finite-time, and strong-coupling regime. With our approach, we can easily work with baths of size up to 300

times the size of the WM with just a standard table-top computer.

The paper is organized as follows. First, in Sec. II, we give a short account on the notions from GQM that will be needed throughout the rest of the paper. This section is intended as an introduction and can be safely omitted by those familiar with GQM. In Sec. III we describe the interaction of the WM with a single bath. In Sec. IV we explore the physics of the Otto cycle, focusing first on the performance of the cycle (Sec. IV A), and then on the dynamics and the role of correlations (Sec. IV B). Finally, we summarize our conclusions in Sec. V. The MATLAB codes of all the numerical computations performed in this work are available at [44].

II. REVIEW OF GAUSSIAN QUANTUM MECHANICS

In this section we review the formalism of Gaussian quantum mechanics, focusing on the aspects necessary for our study. For a much broader and focused introduction to the topic, the reader is referred to Ref. [43].

The primary computational advantages of this formalism are as follows. (i) It allows us to easily study interacting systems via a direct system-plus-bath perspective, rather than relying on open-systems techniques. This lets us study the exact evolution of the bath in addition to the system; a fact we take great advantage of in this work. (ii) Nor do we have to rely on perturbation theory to study such interactions [45].

A. Basics

In GQM, we consider one or more quantum systems ascribed with bosonic canonical quadrature operators, satisfying the canonical commutation relations (CCRs), $[q_i, p_j] = i\delta_{ij}$, where the indices refer to specific bosonic systems (henceforth referred to as oscillators or modes) in our ensemble. If one were to think about an oscillator with Hamiltonian $\frac{p^2}{2m} + \frac{m\omega^2 Q^2}{2}$, then a convenient choice of quadratures would be $q = Q\sqrt{\omega m}$ and $p = \frac{P}{\sqrt{\omega m}}$. In terms of the creation and annihilation operators, the quadratures are expressed through $q_i = (a_i + a_i^\dagger)/\sqrt{2}$ and $p_i = i(a_i^\dagger - a_i)/\sqrt{2}$. For a system of N modes, these quadratures form a phase space that we represent as the vector of operators

$$\mathbf{x} = (q_1, p_1, \dots, q_N, p_N)^T, \quad (1)$$

To reflect the CCRs, this vector satisfies the symplectic structure given by $[x_a, x_b] = i\Omega_{ab}$, where the matrix Ω is called the *symplectic form* and is given by

$$\Omega = \bigoplus_{i=1}^N \begin{pmatrix} 0 & 1 \\ -1 & 0 \end{pmatrix}. \quad (2)$$

In GQM we work with Gaussian states. A state of an N -mode system is Gaussian if and only if it is an exponent of a quadratic form with respect to the coordinates $\{x_a\}_{a=1}^{2N}$. Thermal states (of a quadratic Hamiltonian) fall within this class, and this is the primary reason why we are able to utilize GQM in our study. The defining feature of Gaussian states is that they can be fully described using only their mean position and their variances in phase space. Here all states that we consider will have mean zero (since this is the case for thermal states), and so the formalism further simplifies. We thus characterize the state of our system via the $2N \times 2N$ covariance matrix σ , the entries of which are given by

$$\sigma_{ab} = \langle x_a x_b + x_b x_a \rangle = \text{Tr}[\rho(x_a x_b + x_b x_a)]. \quad (3)$$

A convenient aspect of GQM is that creating ensembles and performing partial traces is trivial. This is due to working in phase space rather than in a Hilbert space, where partitions are represented as a direct sum rather than as a tensor product. Thus, any combined state of two systems A and B takes the form

$$\sigma_{AB} = \begin{pmatrix} \sigma_A & \gamma_{AB} \\ \gamma_{AB}^T & \sigma_B \end{pmatrix}, \quad (4)$$

where σ_A and σ_B are the reduced states of systems A and B respectively, and the matrix γ_{AB} specifies the correlations between the systems. Note that γ_{AB}^T denotes the transposition of the matrix γ_{AB} .

A crucial piece of knowledge needed to work with GQM is that any unitary evolution generated by a time-dependent Hamiltonian that is quadratic at any moment of time will preserve the Gaussianity of a state [46]. Any such unitary operation U on the Hilbert space corresponds to a linear symplectic transformation on the phase space of quadratures: $\mathbf{x} \rightarrow U^\dagger \mathbf{x} U = \mathbf{S}\mathbf{x}$, with \mathbf{S} satisfying

$$\mathbf{S}\Omega\mathbf{S}^T = \mathbf{S}^T\Omega\mathbf{S} = \Omega. \quad (5)$$

The symplecticity of \mathbf{S} (given by Eq. (5)) ensures that the canonical commutation relations are preserved throughout the change of basis. On the level of the covariance matrix, it is easy to see that this transformation acts as

$$\sigma \rightarrow \sigma' = \mathbf{S}\sigma\mathbf{S}^T. \quad (6)$$

B. Energy, Evolution, and Thermality

We are working with zero-mean GQM, and thus we must work with pure quadratic Hamiltonians, H , any example of which can be represented in phase space by a matrix \mathbf{F} defined by $H = \mathbf{x}^T \mathbf{F} \mathbf{x}$. This representation allows us to trivially do the following without ever referencing a Hilbert space object: (i) compute average energies, (ii) evolve the system over time according to some (possibly time dependent) quadratic Hamiltonian,

and (iii) diagonalize the system into its normal mode basis. The methods for these computations are as follows.

The average energy of a state represented by the covariance matrix σ , given the Hamiltonian matrix \mathbf{F} , is given by

$$\langle H \rangle = \frac{1}{2} \text{Tr}(\mathbf{F}\sigma). \quad (7)$$

The symplectic (i.e., unitary in the Hilbert space) evolution matrix $\mathbf{S}(t)$ generated by this (in general, time-dependent) Hamiltonian obeys a Schrödinger-like equation:

$$\frac{d\mathbf{S}(t)}{dt} = \mathbf{\Omega}\mathbf{F}_s(t)\mathbf{S}(t), \quad (8)$$

where $\mathbf{F}_s = \mathbf{F} + \mathbf{F}^T$. For a time-independent evolution, the solution trivially takes the form $\mathbf{S}(t) = \exp(\mathbf{\Omega}\mathbf{F}_s t)$, and for general driven systems, the equation can be straightforwardly integrated by standard numerical techniques.

When speaking of a “free” system, we mean that we are working in the basis that diagonalizes the system’s Hamiltonian (both in Hilbert space and in phase space). For bosonic systems, this is called the normal mode basis, in which the Hamiltonian takes the form

$$H_{\text{free}} = \sum_{i=1}^N \omega_i a_i^\dagger a_i = \sum_{i=1}^N \frac{\omega_i}{2} (p_i^2 + q_i^2), \quad (9)$$

where, in the second equality, we have ignored the (constant) zero-point energy. The corresponding phase-space matrix is diagonal in this basis: $\mathbf{F}_{\text{free}} = \frac{1}{2} \text{diag}(\omega_1, \omega_1, \omega_2, \omega_2, \dots)$. The importance of normal modes is in the fact that, by definition, they do not interact with each other. This means that any thermal state on the entire system is given by the tensor product (in phase space, the direct sum) of the thermal states of each mode individually. A system with interactions will not have this property.

In general, the system may have couplings between pairs of modes (for example, between nearest neighbours), which give non-diagonal elements to the matrix \mathbf{F} . The normal-mode basis can be obtained by symplectically diagonalizing this matrix: $\mathbf{S}\mathbf{F}\mathbf{S}^T = \mathbf{F}_{\text{free}}$. Here \mathbf{S} is the symplectic matrix that transforms to the normal-mode basis, and \mathbf{F}_{free} is diagonal as above.

In the normal-mode basis (i.e., in the basis where the system Hamiltonian takes the form of Eq. (9)), it is straightforward to show that the system’s thermal states are Gaussian, and that their covariance matrices are simply given by

$$\sigma_T = \bigoplus_{i=1}^N \begin{pmatrix} \nu_i^{(T)} & 0 \\ 0 & \nu_i^{(T)} \end{pmatrix}, \quad (10)$$

where

$$\nu_i^{(T)} = 1 + 2 \langle n_i \rangle_T = \frac{\exp(\omega_i/T) + 1}{\exp(\omega_i/T) - 1}. \quad (11)$$

Here ω_i are the normal frequencies and $\langle n_i \rangle_T$ are the average thermal particle numbers. We can thus find the thermal covariance matrix of any interacting system by first identifying the normal basis, specifying the covariance matrix σ as above, and then applying the inverse transformation to this matrix to put it back into the physical-mode basis.

The values $\nu_i^{(T)}$ in Eq. (10) are referred to as the thermal state’s symplectic eigenvalues. Every Gaussian state of N modes has N symplectic eigenvalues ν_i , which are obtained by symplectically diagonalizing the covariance matrix. Specifically, there always exists a symplectic matrix \mathbf{S} such that

$$\mathbf{S}\sigma\mathbf{S}^T = \bigoplus_{i=1}^N \begin{pmatrix} \nu_i & 0 \\ 0 & \nu_i \end{pmatrix}. \quad (12)$$

Note, for example, that σ_T is already diagonalized. From Eq. (11), we see that the symplectic eigenvalues of a ground state, σ_0 , are all equal to one. In fact, the symplectic eigenvalues of a state – which are invariant under symplectic transformations – give a measure of mixedness for that state. For example, a Gaussian state is pure if and only if all its symplectic eigenvalues are equal to one, and no state can have any eigenvalues smaller than one (this is a statement of the uncertainty principle).

For this reason, often we do not focus directly on the diagonalizing transformation of a state but rather just its symplectic eigenvalues. These can be easily computed by taking the regular eigenvalues of the matrix $i\mathbf{\Omega}\sigma$, which come in $\pm\nu_i$ pairs.

C. Entropy and Correlations

In this study we compute the distribution and evolution of correlations between the parties in our heat engine. Consider a two-party state of the form Eq. (4). The off-diagonal matrix γ_{AB} contains the correlation functions between the two systems, and these systems are uncorrelated if and only if all elements are zero.

For this purpose, we use the mutual information as our correlation measure, defined as

$$I(A, B) = S(\sigma_A) + S(\sigma_B) - S(\sigma_{AB}), \quad (13)$$

where here $S(\sigma)$ is the von Neumann entropy of the state with covariance matrix σ . As stated above, the symplectic eigenvalues of a Gaussian state specify how mixed that state is. This can be quantified exactly, in that the entropy takes the form

$$S(\sigma) = \sum_{i=1}^N f(\nu_i), \quad (14)$$

where

$$f(x) = \frac{x+1}{2} \log\left(\frac{x+1}{2}\right) - \frac{x-1}{2} \log\left(\frac{x-1}{2}\right). \quad (15)$$

We are thus able to very easily compute the mutual information across any partition in our system, independent of how many modes each partition contains.

Note that the entanglement is also computable, but, for most situations, it is considerably more difficult. In the case of two modes it is very easy [47], and we discuss some findings in that regard in the next sections. However, due to the thermality of our system, quantum correlations are hard to maintain and we have found that generally entanglement does not play a significant role in the scenarios we consider below. Interestingly, this aspect is in accord with (yet by no means logically necessitated by) the fact that, although capable of manifesting many interesting quantum features, GQM is an essentially classical, noncontextual sector of quantum mechanics in that it can be described by a local hidden variable model [48].

III. GAUSSIAN INTERACTION WITH A SINGLE BATH

Before performing the analysis of the Otto cycle, let us study some relevant features of the isochoric interaction of the WM with a single thermal bath. We will thereby introduce the specific Hamiltonians that describe the components of the Otto engine in the next sections.

Throughout this work we model thermal baths as collections of harmonic oscillators arranged in one-dimensional, translation-invariant rings with nearest-neighbour interactions. We consider only position-position couplings so that the free Hamiltonian of a bath is given by

$$H_{\text{bath}} = \sum_{i=1}^N \frac{\omega_b}{2} (p_i^2 + q_i^2) + \sum_{i=1}^N \alpha q_i q_{i+1}, \quad (16)$$

where N is the number of oscillators in the bath, ω_b is the bare frequency of each of them, and α controls the coupling strength. Note that, because of the periodic boundary conditions, $q_{N+1} = q_1$.

The phase-space matrix corresponding to this Hamiltonian is

$$\mathbf{F}_{\text{bath}} = \frac{1}{2} \begin{pmatrix} \omega_b & \alpha & \mathbf{0} & \cdots & \mathbf{0} & \alpha \\ \alpha & \omega_b & \alpha & \cdots & \mathbf{0} & \mathbf{0} \\ \vdots & \vdots & \vdots & \ddots & \vdots & \vdots \\ \alpha & \mathbf{0} & \mathbf{0} & \cdots & \alpha & \omega_b \end{pmatrix}, \quad (17)$$

where $\mathbf{0}$ is the 2×2 matrix of zeros, and

$$\omega_b = \begin{pmatrix} \omega_b & 0 \\ 0 & \omega_b \end{pmatrix}, \quad \alpha = \begin{pmatrix} \alpha & 0 \\ 0 & 0 \end{pmatrix}. \quad (18)$$

At the beginning of the process, the bath is initialized in a thermal state $\rho(0) \propto e^{-H_{\text{bath}}/T_b}$ at temperature T_b .

Due to the interactions, the covariance matrix will *not* be given by a simple direct sum as in Eq. (10). Rather, we must first identify the normal mode basis

that symplectically diagonalizes the Hamiltonian matrix $\omega_{\text{bath}}/2 = \mathbf{S}\mathbf{F}_{\text{bath}}\mathbf{S}^T$, where ω_{bath} is the diagonal matrix composed of the normal mode frequencies of H . We then identify the thermal state as per Eq. (10) and finally transform back to the physical basis to find the thermal state of the ring, $\sigma_{\text{bath}} = S^{-1}\sigma_T(S^T)^{-1}$ (this calculation is included in the function *Initialize* in Ref. [44]).

As a WM we employ yet another harmonic oscillator, with bare frequency ω_m . Its coupling to the bath is described by

$$H_{\text{int}} = \gamma \lambda(t) q_m \sum_{i \in \{\text{int}\}} q_i \quad (19)$$

where $\{\text{int}\}$ is the set of the bath's nodes which the WM interacts with.

For most of our analysis we choose this set to contain just one and always the same node of the bath, which we label to be the first node q_1 . However, a situation where the interaction set has more than one element is discussed in Sec IV A.

The function $\lambda(t)$ is a *switching function* that modulates the interaction in time. In particular, we choose the following compactly-supported, smooth switching function

$$\lambda(t) = \begin{cases} 0 & t < 0 \\ \frac{1}{2} - \frac{1}{2} \tanh \cot \frac{\pi t}{\delta} & 0 \leq t < \delta \\ 1 & \delta \leq t < \tau - \delta \\ \frac{1}{2} + \frac{1}{2} \tanh \cot \frac{\pi(t-\tau)}{\delta} & \tau - \delta \leq t < \tau \\ 0 & t > \tau \end{cases}, \quad (20)$$

where $\tau \geq 2\delta$ is the total duration of the interaction with the bath and δ is the time that takes to fully switch on (and fully switch off) the interaction.

The phase-space matrix of the overall Hamiltonian will then be $\mathbf{F}_{\text{tot}} = \begin{pmatrix} \frac{1}{2}\omega_m & \frac{1}{2}\gamma \\ \frac{1}{2}\gamma^T & \mathbf{F}_{\text{bath}} \end{pmatrix}$. Here γ is a $2 \times 2N$ matrix containing all zeros except for the first entry $\gamma_{11} = \lambda(t)\gamma$, corresponding to the $q_m q_1$ interaction we are imposing.

We desire the symplectic evolution matrix $\mathbf{S}(t)$ that will tell us how the system evolves. This matrix satisfies the equation of motion (8). Here we use \mathbf{F}_{tot} and numerically integrate Eq. (8) to solve for $\mathbf{S}(t)$. To evolve the state, we simply apply this matrix to our initial covariance matrix: $\sigma_{\text{tot}}(t) = \mathbf{S}(t)(\sigma_m \oplus \sigma_{\text{bath}})\mathbf{S}(t)^T$, where here $\sigma_m = \text{diag}(\nu^{(m)}, \nu^{(m)})$ is the initial state of the WM, its values given by Eq. (11). This process can be explicitly found in various files in the computational appendix [44].

During the evolution of the WM+bath system we have found that the state of the WM remains very close to being thermal, this is, that its covariance matrix is very close to that given by Eq. (10) for some $\nu^{(T)}$ (for a more detailed discussion and an explicit characterization of the distance of the actual state of the WM to a thermal state, see appendix A). Given this, we are able to assign a meaningful effective temperature to the WM by computing the

temperature associated with its symplectic eigenvalue. An example of this is shown by the green, dashed line of Fig. 1. Note that, at the end of the process, the system is exactly thermal and at the temperature of the bath.

Before continuing, let us explain our choice of parameters, which is not accidental. We found during the course of our study that the WM best thermalizes with the baths if we match the frequencies so that ω_m is also the frequency of the individual bath oscillators, i.e., the frequencies in Eq. (16). Similarly, we discover that thermalization is best achieved when we also match the interaction strength with the ring coupling strength, i.e., when $\gamma = \alpha$. Indeed, in this case, the WM can be thought of as interacting with the oscillators in the bath *on equal footing*, ensuring that the rate of transfer of heat and information between the WM and the bath is the same as between oscillators in the bath itself. Due to this, we will from now on set $\omega_m = \omega_b$ and $\gamma = \alpha$.

Importantly, due to finite speed and finite strength of WM-bath interaction, the above thermalization process has a non-zero work cost. More specifically, the extracted work, as quantified by the difference between the initial and final average energies of the total system, is non-zero. However, despite the strong non-equilibrium character of the process, this amount is small (compared to, e.g., the energy exchanged between the WM and the bath). For example, for $N = 30$, $\gamma = \alpha = 0.1$, $\omega_m = \omega_b = 2$, $T_b = 4$, and $\tau = 100$, with the ramp-up time being $\delta = 0.1\tau$, the relaxation work is only 2×10^{-3} . This, together with the fact of exact thermalization discussed above, means that the fine-tuning of the frequencies and couplings provides us with an example of exact, almost work-free thermalization in finite time, resulting from a strong interaction between the WM and the bath. A similar example, where the structure of the bath is known and the Hamiltonian of the WM is finely-tuned, was constructed in [49]. This is not a standard, exponential relaxation behaviour [42], and it can be argued that such behaviour cannot occur for general baths of unknown structure [23]. Furthermore, the fact of almost zero work justifies the usage of the term ‘‘isochoric’’ for this process. Indeed, in this case, most of the energy exchange is heat transfer, which is the characteristic of isochoric processes [12]. In the strong coupling regime, strictly isochoric (or equivalently, constant-Hamiltonian processes) cannot exist as any non-zero coupling will change the system Hamiltonian, and therefore the term needs to be adapted.

Furthermore, subtle processes such as the evolution of the correlations between the WM and the bath or information exchange between the WM and the bath can be examined in very great detail within the framework of GQM. As an illustration, in Fig. 1 we also examine the evolution of the correlations between various partitions during the interaction.

We compare the correlations, as measured by the mutual information, between the WM and the whole bath (solid blue line), between the WM and the node in the bath it interacts with (black dotted line), and between

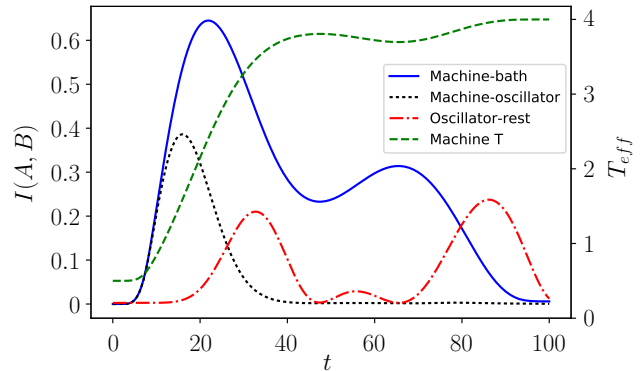


FIG. 1. Evolution of several quantities during a period of interaction between the working body and a thermal bath. The green dashed line is the working body effective temperature. The other lines represent the mutual information between various partitions: (solid blue) between the machine and the bath as a whole, (black dotted) between the machine and the specific bath oscillator with which it interacts, and (red dot-dashed) between this oscillator and the rest of the bath. The bath contains $N = 30$ oscillators all with frequency $\omega_b = 2$, and is initialized in a thermal state at temperature $T_b = 4$. The machine has also frequency $\omega_m = \omega_b$, but is initialized in a thermal state at temperature $T_m = 0.5$. The total time of interaction is $\tau = 100$, the ramp-up time is $\delta = 0.1\tau$ and the interaction strengths are $\alpha = \gamma = 0.1$. Note that the red curve is not initially zero (it should not be, because there is initial correlation from the ring couplings). However, since we are working with a relatively hot bath, these correlations are very small (of the order of 10^{-3}), and its magnitude cannot be appreciated in full detail in the plot.

the latter and the rest of the bath (red dot-dashed line). This provides us with a number of insights into the non-perturbative interaction of the WM and the bath. First, we see that during the phase of switching on the interaction the WM and the bath quickly build up strong correlations, which typically decay later on. This decay is caused by the fact that the bath nodes to which the WM is coupled also interact with the rest of the bath, and the bath, due to its tendency to thermalize, forces these correlations to decay. We can see this process in more detail by examining the other two lines. The correlation between the machine and the interacting node similarly rises and then falls, and the decay occurs exactly as this node becomes significantly correlated with the rest of the bath.

This gives us an important intuitive picture. The interaction between the WM and the bath generates correlations between the two (specifically, between the WM and the interacting node). Due to the intra-bath couplings, the WM also becomes correlated with other ring nodes in an outwards-propagating manner. However, these couplings also mean that the correlation between the WM and bath will, over time, be swapped to correlations between different bath nodes, as we see, for example, in the

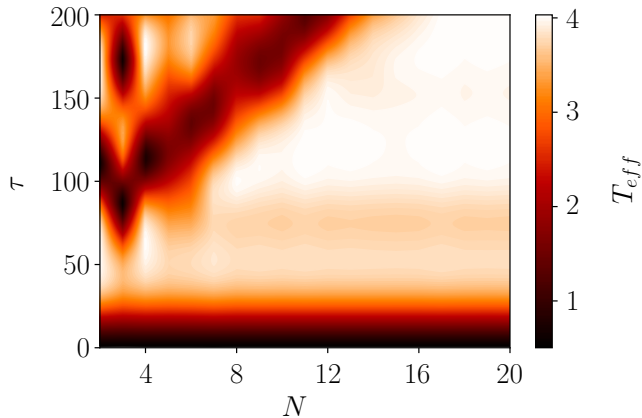


FIG. 2. Effective temperature of the WM after the interaction with the bath as a function of the bath size N and the time of interaction τ . The parameters for the WM are those used also for Fig. 1 ($\omega_m = 2$, $T_m = 0.5$), and similarly for the relevant parameters of the bath ($\omega_b = 2$, $T_b = 4$, $\alpha = \gamma = 0.1$). The ramp-up time of the interaction is $\delta = 0.1\tau$ for every value of τ . Note the two distinct behaviors separated by a straight line $\tau = c \cdot N$.

red dot-dashed line in Fig. 1. Over the course of many interaction sessions, the bath modes therefore become more and more intercorrelated, which will eventually result in a halt of the machine. We elaborate on this process in the next section, where we discuss the performance of a WM operating cyclically between two finite-sized baths.

One does not need to move to the two-bath scenario to observe the effects of having finite baths, though. In fact, one only needs to interact with the bath for a time that is long enough. We do so in Fig. 2, where we compute the effective temperature of the machine after interacting with a bath composed of N nodes during a time τ , for different values of N and τ , and all the other parameters being the same as those used for Fig. 1.

In Fig. 2, we observe two very distinct behaviors that are clearly separated. For $\tau < c \cdot N$, where c indicates the slope of the “light cone”, the temperature of the WM is insensitive to the size of the bath. Indeed, the interaction time in this case is short enough so as to allow the interaction to finish before the perturbations that propagate through the bath return to the region which interacts with the WM (i.e., the interacting node of the ring). Therefore, there is no difference between the temperature that the WM achieves in this case and the temperature that it would achieve from interacting with an infinite bath. The opposite occurs for $\tau > c \cdot N$: in this case, the interaction time is long enough so as to permit the perturbations generated by the interaction with the WM to return to the interacting node. These perturbations modify the local state of the interacting node, which in turn translates into a response in the WM that diverges from that expected for infinite baths.

It is also worth noting that for short interaction times

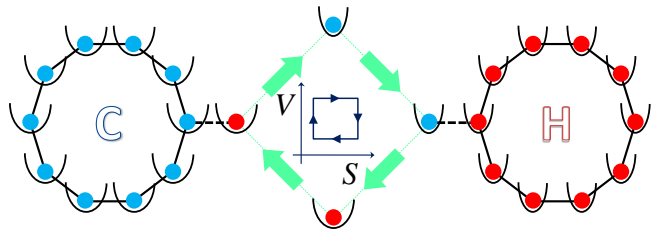


FIG. 3. Visualization of the Otto cycle. The standard sequence of isochoric thermalisations and adiabatic compressions/expansions defining the Otto cycle in phenomenological thermodynamics are, in our case, implemented as a sequence of $q - q$ interactions (as in Sec. III) and sudden quenches of the WM’s potential. More specifically, the cycle consists of the following steps: (i) the WM interacts with the hot bath (the red harmonic chain) by a coupling that is smoothly switched on, kept constant, and smoothly switched off, (ii) the frequency of the WM is suddenly quenched to match the individual frequencies in the cold bath, (iii) the WM is brought into contact with the cold bath (the blue harmonic chain), with the same pattern of interaction as in step (ii), and (iv) the frequency of the WM is suddenly quenched back to the frequency of an individual oscillator in the hot bath.

the WM does not have enough time to fully thermalize with the bath. We observe that the effective temperature of the WM increases with the interaction time until the point where thermalization is achieved. After this point, increasing the interaction time further has no major influence on the WM’s temperature (until, of course, it is long enough for the perturbations to go around the bath).

IV. THE GAUSSIAN OTTO CYCLE

We now study the performance of the WM running an Otto cycle between two thermal baths at temperatures T_h (hot) and T_c (cold), as depicted in Fig. 3.

The Otto cycle we consider is composed of two isochoric interactions between the machine and each of the baths (as described in Sec. III) separated by two instantaneous quenches of the WM’s Hamiltonian. That is, between subsequent interactions, we abruptly change the frequency of the WM,

$$H_m = \omega_c a_m^\dagger a_m \leftrightarrow H'_m = \omega_h a_m^\dagger a_m, \quad (21)$$

so that the WM’s state remains unchanged. The fact that the system is detached from the baths during the quench ensures that the process is adiabatic in the thermodynamic sense [50]. Here, ω_c and ω_h are the frequencies of the WM used during the interactions with the cold and hot baths, respectively. As mentioned in Sec. III, ω_c and ω_h are chosen to coincide with the frequencies of the nodes of, respectively, the cold and the hot baths. Moreover, we also match the interaction strength with the ring

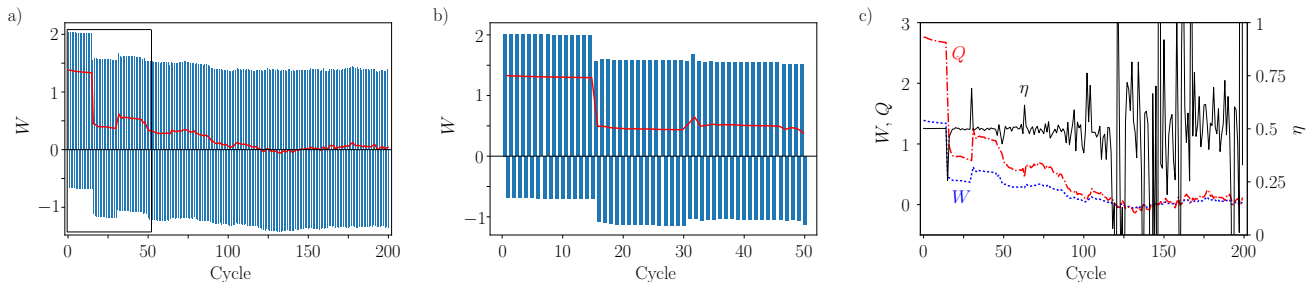


FIG. 4. a) Work output after each quench of the machine oscillator. One pair of positive-negative bars represents a full cycle. The red, solid line represents the total work extracted from each cycle (positive bar + negative bar). The relevant parameters of the system are $N_h = N_c = 300$, $T_h = 4$, $T_c = 0.5$, $\omega_h = 2$, $\omega_c = 1$, $\alpha_h = \alpha_c = \gamma = 0.1$, $\tau = 100$, $\delta = 0.1\tau$. b) Zoom-in on the box in Figure (a). c) (Dotted blue) Work output, (dot-dashed red) heat loss in the hot bath, and (solid black) efficiency for every cycle of operation. Note the divergences in the efficiency caused by the extraction of no heat from the hot bath.

coupling strengths, i.e., $\gamma = \alpha_c = \alpha_h$ (we choose $\alpha_c = \alpha_h$ for simplicity only, without losing generality). This ensures that the WM thermalizes with the baths and that the rate of heat and information transfer between the machine and the baths is the same as that among the oscillators within the baths.

The total work extracted during a cycle is given by the sum of works extracted during each of the four parts of the cycle. As we showed in Sec. III, the work contributions from WM-bath interactions are small, hence most of the work is generated during the quenches. The work produced by a quench is given by a particularly simple expression. Indeed, since the baths remain intact during the quench, the work is given by the energy change of the WM. For example, for the quench after an interaction with the hot bath, the energy of the WM is decreased by $W_{h \rightarrow c} = (\omega_h - \omega_c) \text{Tr} \sigma_m$. If we choose $\omega_c < \omega_h$, not only will $W_{h \rightarrow c} > 0$, but also the net work will be positive. Note also that if $\omega_c > \omega_h$ we would be running a refrigerator. Lastly, note that the engine cycles are not cyclic in the traditional sense. Indeed, since the baths are finite, at the end of each cycle, the state of the WM will be different from that at the beginning.

A. Cycle performance

We begin the cycle by the interaction with the hot bath, so the initial state of the machine is chosen to be a thermal state at temperature T_c and with frequency ω_h . Due to the finite size of the baths we expect that, over time, the performance of the engine will drop. This intuition is confirmed in Fig. 4, where we plot the work output, heat, and efficiency of the engine as a function of cycle numbers. In Figs. 4a and 4b, each bar represents the sum of the work in a quench and the work in the isochore preceding the quench, as described above. The heat Q is defined as the energy the hot bath loses per cycle. We define the energy of the bath with respect to the Hamiltonian in Eq. (16), and, for the n -th cycle, the

heat is given by

$$Q = -\Delta E_h = \text{Tr} [\mathbf{F}_{\text{bath}}(\sigma_h(2n\tau) - \sigma_h((2n+1)\tau))], \quad (22)$$

where $\sigma_h(t)$ is the covariance matrix describing the state of the hot bath as a function of time. The efficiency of the engine is defined as usual: $\eta = W/Q$.

The first important implication of Fig. 4 is that, during the first several cycles of operation, the machine extracts work at a constant rate, with the efficiency $\eta_O = 1 - \omega_c/\omega_h$. The latter is the theoretical maximum for an oscillator running an idealized Otto cycle between two infinite thermal baths to which it is coupled weakly enough for the standard Markovian open quantum system techniques [42] to be applicable [51, 52]. However, in striking contrast to the idealized engine, which achieves the maximal efficiency only at zero power, our engine produces non-zero work and does so in finite time, thereby producing non-zero power. What is more, during these first cycles, the perturbations, created by the interaction with the WM, propagate through the bath in the same way as they would do if the bath were infinite. Once these perturbations travel past the interacting node, it locally appears the same as if the bath were in a thermal state again. Thus, for infinite baths, our engine can run at this (maximal) efficiency for an arbitrary number of cycles.

In Fig. 4, we see that the work output is approximately constant for the first 15 complete cycles. Differences from the ideal behavior begin to appear only when the perturbations return to the region of the bath that directly interacts with the WM. This is the point at which the finite size of the baths starts having a detrimental impact on the functioning of the engine, and it is marked by the drastic, discontinuous drop in the work output in Fig. 4.

We observe that the number of ideal cycles increases linearly with $N \equiv N_c = N_h$, the number of nodes in the baths, as is to be expected given the finite speed of propagation of the perturbations in the bath. Recall that, for nearest-neighbour Hamiltonians such as that in Eq. (16), the Lieb-Robinson bounds set limitations on the propagation of perturbations [14, 15]. Therefore,

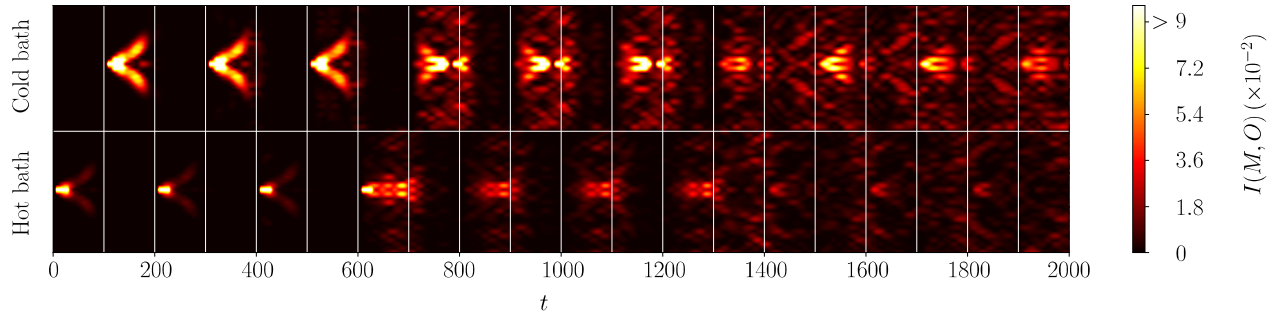


FIG. 5. Mutual information between the WM and each oscillator in each bath during 10 cycles of operation. The horizontal line separates the two baths, and the vertical lines separate the interactions of the machine with each of the baths. The baths have $N = 30$ oscillators each, and are initially uncorrelated and at temperatures $T_c = 0.5$ and $T_h = 4$. Note how during the first three cycles the machine observes no differences from the interaction with infinite baths, and after this point the perturbations in the chains arrive back to the interacting oscillator, modifying its local state.

the total work the engine can extract from the baths grows asymptotically linearly with the size, as given by the number of constituents, of the baths.

As an aside, we also considered coupling the WM to more than one, evenly spaced ring sites. It turns out that adding more interacting sites reduces the amount of initial ideal cycles, which matches the intuitive picture described above. Indeed, the reduced distance between the sites leads to shorter time needed for the perturbations created by the interaction to reach the nearest site of interaction. Interestingly, the work output of just one cycle during ideal performance is insensitive to the cardinality of the set $\{\text{int}\}$ (as long as the perturbations generated in one interacting site do not have time to arrive to any other), but of course the total work output of the engine over several cycles does get reduced by increasing the interaction points. On the other hand, the more interaction sites we take, the smaller is the time necessary for the system to thermalize. This leads to an increased power output for the initial ideal cycles, albeit at the cost of decreasing the number of such cycles.

Lastly, we have studied the influence on our engine of the ramp-up time $\delta \leq \tau/2$, which is the time taken to switch the interaction completely on or off. Non-commutative time-dependent interaction terms usually generate excitations causing thermodynamic friction (see, e.g., [25, 51, 53]), and thus the rate of switching can be expected to have a significant impact on the engine's performance. However, in our current scenario, we found that the dependence on δ is negligible compared to the energy scale of the engine as a whole, even in the limit of very sharp switching.

B. Propagation of correlations

The formalism presented in Sec. II allows, as noted before, an easy way of identifying whether two systems

are correlated. In this subsection, we use this property to study how correlations distribute along the baths and the WM. We consider this as one of the (probably many) paths to a better intuitive understanding of the phenomenology presented above.

In Fig. 5 we show the strength of the correlations between the WM and each of the oscillators in each bath and how these correlations evolve in time for 10 consecutive cycles of operation of the machine. In this case, and throughout this subsection, each bath is composed of $N = 30$ oscillators, all other parameters being the same as in the preceding sections. The vertical lines denote the instants at which the machine stops interacting with one bath and, after the corresponding quench, begins interacting with the other.

One feature we immediately observe is the explicit propagation of the perturbations in the form of localized wavepackets at finite speed, in full agreement with the Lieb-Robinson bound [14, 15]. Interestingly, during the first three cycles of operation ($t \in [0, 600]$), the WM appears to interact with unperturbed baths. These are the cycles in which the infinite-size bath approximation is valid and the work output is optimal, as in the initial cycles in Fig. 4. The time $t = 600$ is when the perturbations that were generated during the first interactions with the bath manage to intercept the WM as it is *currently interacting* with the bath, leading to the sudden drop of the work output that has been discussed in Sec. IV A.

We also see that the propagating correlations quickly fade. This is unsurprising, and carries the same explanation as that given for Fig. 1. Our computations show that, to a surprisingly good approximation, during an interaction the WM becomes correlated with just a single non-local mode in the bath—the mode that propagates outwards—as can be appreciated in Fig. 5. However, both the WM and this propagating mode are interacting with the rest of the bath as well, and thus this correlation is quickly lost and distributed among bath modes.

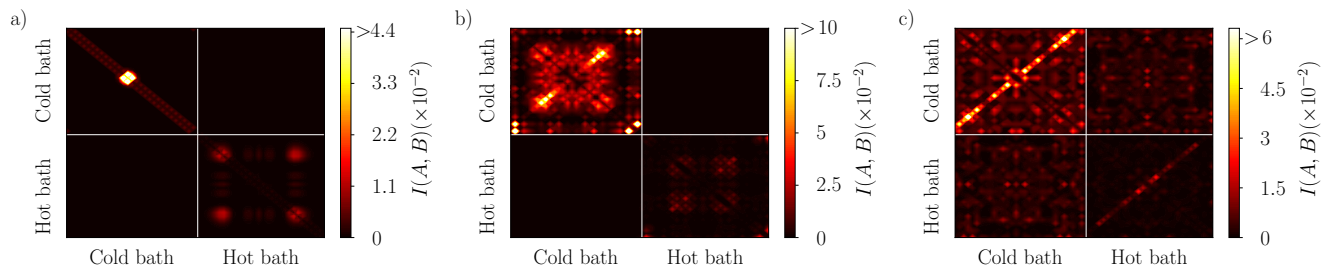


FIG. 6. Bath-bath correlations in different moments of time: a) $t = 1.2\tau$, i.e., during the first interaction with the cold bath after the initial interaction with the hot bath (note that the correlations are propagating outwards, away from the interaction point), b) $t = 6\tau$, i.e., after the third interaction with the cold bath, and c) $t = 12.5\tau$, i.e., during the interaction with the hot bath after performing six full cycles of operation.

This also explains why the decay occurs much faster in the hot bath than in the cold bath. Indeed, the hotter the bath, the larger the thermal noise that will break the correlations.

It is also interesting to see how the correlations are built up and distributed along the baths (and between them) over time. Given that the WM acts as a carrier of both energy and correlations between the baths, one would expect that over time the baths get correlated and end up reaching a global passive state. We explore this intuition in Fig. 6, in which we show the mutual information between every pair of oscillators in any bath for various times. The code for generating a full animation of the evolution of the correlations is included in the script *correlations* in the computational appendix [44]. This animation shows how correlations propagate at constant speed through the baths. During the first cycles of interaction the bath-bath correlations are very weak and short-lived, and it is not until the fourth cycle that they become comparable to the intra-bath correlations.

It is worth noticing that despite the fact that the mutual information between different elements of the system can be substantially large, for our choice of parameters none of the correlations built involve entanglement. Indeed, it is well known that entanglement in quantum fields decays very rapidly with temperature, reaching zero at a finite value [47]. However, for a sufficiently cold bath, one could still expect some entanglement to be present, although it is not clear whether it will play a significant role in the engine's performance.

V. SUMMARY AND CONCLUSIONS

Using the formalism of Gaussian quantum mechanics we have been able to circumvent the standard assumptions of weak coupling, slow driving, and infinite size of the baths, usually employed in studying thermodynamic phenomena. The focus of our study was on a single driven harmonic oscillator undergoing an Otto cycle between two finite harmonic thermal reservoirs. Despite the attention the physics beyond these assumptions has

received in recent years, to the best of the authors' knowledge this is the first work where none of these assumptions is made.

We first study the interaction of a machine with a single bath, modeled as an N -node translationally-invariant harmonic ring. GQM allows to observe not only how the machine thermalizes, but also how the interaction creates correlations between the WM and the region of the bath that directly interacts with it, and how these correlations later on propagate across the bath. If the interaction is long enough, perturbations formed at the beginning can reach around the chain and disrupt the machine's final thermal state.

In our study of the quantum Otto cycle we conclude that the crucial element that determines the performance of the cycle is the propagation of the perturbations created by the WM-bath interaction. During the first cycles of operation the WM interacts with a locally ideal state of the baths and therefore an ideal, infinite-sized-baths behaviour is observed. However, during these interactions perturbations are being generated, which propagate through the baths as wavepackets. After enough time these perturbations return to the interaction region and start disrupting the thermalization of the WM, affecting the work output and efficiency of the machine.

The number of cycles of ideal performance can be increased by decreasing the interaction time between the WM and baths. Each interaction, however, needs to be long enough to allow for equilibration of the WM. The time needed could be reduced by increasing the interaction strength γ , but at the cost of creating larger perturbations in the bath. Finding the optimal value of γ to balance these factors may prove very fruitful.

We have also explored the interplay between the degradation of our engine and the creation of correlations within the baths. As discussed, the process of running the engine inevitably creates an increasing number of correlations with the baths, within the baths, and among the baths. This represents the system's gradual evolution to a more and more passive state. We believe that further study into this dynamics is warranted.

The objective of this work is to demonstrate the ca-

pabilities of Gaussian quantum mechanics as a means of assessing finite-size effects in a field that has historically relied on infinite (time, size, and subtlety of the interactions) idealizations. Not only can GQM address fundamental questions in quantum thermodynamics, but it also provides us with more tractable numerical computations. This we believe may be of great use for the community of quantum thermodynamics.

ACKNOWLEDGMENTS

A. P.-K. gratefully acknowledges Fundación Obra Social “la Caixa” for their support. The work of K. V. H. was supported by the Villum Fonden. E. G. B. acknowledges the support of the Natural Sciences and Engineering Research Council of Canada. All authors acknowledge financial support from the Spanish MINECO (QIBEQI FIS2016-80773-P and Severo Ochoa SEV-2015-0522), Fundació Privada Cellex and the Generalitat de Catalunya (SGR875 and CERCA Program).

-
- [1] L. Landau and E. Lifshitz, *Statistical Physics, Part I* (Pergamon, New York, 1980).
- [2] R. Alicki, *The quantum open system as a model of the heat engine*, J. Physics A: Math. Gen. **12**, L103 (1979).
- [3] K. Sekimoto, F. Takagi, and T. Hondou, *Carnot’s cycle for small systems: Irreversibility and cost of operations*, Phys. Rev. E **62**, 7759 (2000).
- [4] N. Shiraishi, K. Saito, and H. Tasaki, *Universal trade-off relation between power and efficiency for heat engines*, Phys. Rev. Lett. **117**, 190601 (2016).
- [5] D. Reeb and M. M. Wolf, *An improved Landauer principle with finite-size corrections*, New J. Phys. **16**, 103011 (2014).
- [6] M. P. Woods, N. Ng, and S. Wehner, *The maximum efficiency of nano heat engines depends on more than temperature*, arXiv:1506.02322 [quant-ph].
- [7] H. Tajima and M. Hayashi, *Finite-size effect on optimal efficiency of heat engines*, Phys. Rev. E **96**, 012128 (2017).
- [8] J. G. Richens, Á. M. Alhambra, and L. Masanes, *Finite-bath corrections to the Second law of thermodynamics*, arXiv:1702.03357 [quant-ph].
- [9] H. E. D. Scovil and E. O. Schulz-DuBois, *Three-level masers as heat engines*, Phys. Rev. Lett. **2**, 262 (1959).
- [10] E. Geva and R. Kosloff, *A quantum-mechanical heat engine operating in finite time. A model consisting of spin-1/2 systems as the working fluid*, J. Chem. Phys. **96**, 3054 (1992).
- [11] J. Rossnagel, S. T. Dawkins, K. N. Tolazzi, O. Abah, E. Lutz, F. Schmidt-Kaler, and K. Singer, *A single-atom heat engine*, Science **352**, 325 (2016).
- [12] H. Callen, *Thermodynamics and an Introduction to Thermostatistics*, 2nd ed. (John Wiley, 1985).
- [13] Whenever we refer to “infinitely large” systems, we mean finite systems that are so large that their finiteness cannot be observed within the largest timescale involved in the discussion.
- [14] B. Nachtergaele, H. Raz, B. Schlein, and R. Sims, *Lieb-Robinson bounds for harmonic and anharmonic lattice systems*, Commun. Math. Phys. **286**, 1073 (2009).
- [15] B. Nachtergaele and R. Sims, *Lieb-Robinson bounds in quantum many-body physics*, Contemp. Math. **529**, 141 (2010), arXiv:1004.2086.
- [16] L. Masanes and J. Oppenheim, *A general derivation and quantification of the Third law of thermodynamics*, Nat. Commun. **8**, 14538 (2017).
- [17] H. B. Reitlinger, *Sur l’utilisation de la chaleur dans les machines à feu* (Vaillant-Carmanne, Liège, Belgium, 1929).
- [18] F. L. Curzon and B. Ahlborn, *Efficiency of a Carnot engine at maximum power output*, Am. J. Phys. **43**, 22 (1975).
- [19] C. V. den Broeck, *Thermodynamic efficiency at maximum power*, Phys. Rev. Lett. **95**, 190602 (2005).
- [20] A. E. Allahverdyan, R. S. Johal, and G. Mahler, *Work extremum principle: Structure and function of quantum heat engines*, Phys. Rev. E **77**, 041118 (2008).
- [21] U. Seifert, *Efficiency of autonomous soft nanomachines at maximum power*, Phys. Rev. Lett. **106**, 020601 (2011).
- [22] L. A. Correa, J. P. Palao, G. Adesso, and D. Alonso, *Performance bound for quantum absorption refrigerators*, Phys. Rev. E **87**, 042131 (2013).
- [23] A. E. Allahverdyan, K. V. Hovhannisyanyan, A. V. Melkikh, and S. G. Gevorgian, *Carnot cycle at finite power: Attainability of maximal efficiency*, Phys. Rev. Lett. **111**, 050601 (2013).
- [24] A. del Campo, J. Goold, and M. Paternostro, *More bang for your buck: Super-adiabatic quantum engines*, Sci. Rep. **4**, 6208 (2014).
- [25] F. Plastina, A. Alecce, T. J. G. Apollaro, G. Falcone, G. Francica, F. Galve, N. Lo Gullo, and R. Zambrini, *Irreversible work and inner friction in quantum thermodynamic processes*, Phys. Rev. Lett. **113**, 260601 (2014).
- [26] F. Binder, S. Vinjanampathy, K. Modi, and J. Goold, *Quantacell: powerful charging of quantum batteries*, New J. Phys. **17**, 075015 (2015).
- [27] G. Benenti, G. Casati, K. Saito, and R. Whitney, *Fundamental aspects of steady-state conversion of heat to work at the nanoscale*, Phys. Repts. **694**, 1 (2017).
- [28] R. Gallego, A. Riera, and J. Eisert, *Thermal machines beyond the weak coupling regime*, New J. Phys. **16**, 125009 (2014).
- [29] N. Freitas and J. P. Paz, *Analytic solution for heat flow through a general harmonic network*, Phys. Rev. E **90**, 042128 (2014).
- [30] D. Gelbwaser-Klimovsky and A. Aspuru-Guzik, *Strongly coupled quantum heat machines*, J. Phys. Chem. Lett. **6**, 3477 (2015).
- [31] M. Esposito, M. A. Ochoa, and M. Galperin, *Quantum Thermodynamics: A Nonequilibrium Green’s Function Approach*, Phys. Rev. Lett. **114**, 080602 (2015).
- [32] U. Seifert, *First and Second law of thermodynamics at strong coupling*, Phys. Rev. Lett. **116**, 020601 (2016).

- [33] R. Uzdin, A. Levy, and R. Kosloff, *Quantum Heat Machines Equivalence, Work Extraction beyond Markovianity, and Strong Coupling via Heat Exchangers*, Entropy **18**, 124 (2016).
- [34] P. Strasberg, G. Schaller, N. Lambert, and T. Brandes, *Nonequilibrium thermodynamics in the strong coupling and non-Markovian regime based on a reaction coordinate mapping*, New J. Phys. **18**, 073007 (2016).
- [35] D. Newman, F. Mintert, and A. Nazir, *Performance of a quantum heat engine at strong reservoir coupling*, Phys. Rev. E **95**, 032139 (2017).
- [36] M. Perarnau-Llobet, H. Wilming, A. Riera, R. Gallego, and J. Eisert, *Fundamental corrections to work and power in the strong coupling regime*, arXiv:1704.05864 [quant-ph].
- [37] A. E. Allahverdyan, K. V. Hovhannisyan, D. Janzing, and G. Mahler, *Thermodynamic limits of dynamic cooling*, Phys. Rev. E **84**, 041109 (2011).
- [38] J. P. Pekola, S. Suomela, and Y. M. Galperin, *Finite-size bath in qubit thermodynamics*, J. Low Temp. Phys. **184**, 1015 (2016).
- [39] J. Scharlau and M. P. Müller, *Quantum Horn's lemma, finite heat baths, and the Third law of thermodynamics*, arXiv:1605.06092 [quant-ph].
- [40] A. Caldeira and A. Leggett, *Quantum tunnelling in a dissipative system*, Annals of Physics **149**, 374 (1983).
- [41] U. Weiss, *Quantum dissipative systems*, 2nd ed. (World Scientific, 1999).
- [42] H.-P. Breuer and F. Petruccione, *The theory of open quantum systems* (Oxford University Press, 2002).
- [43] G. Adesso and F. Illuminati, *Entanglement in continuous-variable systems: recent advances and current perspectives*, J. Phys. A: Math. Theor. **40**, 7821 (2007).
- [44] A. Pozas-Kerstjens, K. V. Hovhannisyan, and E. G. Brown, *Computational appendix of a quantum Otto engine with finite heat baths: energy, correlations, and degradation*, GitHub repository (2017).
- [45] E. G. Brown, E. Martín-Martínez, N. C. Menicucci, and R. B. Mann, *Detectors for probing relativistic quantum physics beyond perturbation theory*, Phys. Rev. D **87**, 084062 (2013), arXiv:1212.1973.
- [46] B. L. Schumaker, *Quantum mechanical pure states with gaussian wave functions*, Phys. Repts. **135**, 317 (1986).
- [47] E. G. Brown, *Thermal amplification of field-correlation harvesting*, Phys. Rev. A **88**, 062336 (2013).
- [48] S. D. Bartlett, T. Rudolph, and R. W. Spekkens, *Reconstruction of Gaussian quantum mechanics from Liouville mechanics with an epistemic restriction*, Phys. Rev. A **86**, 012103 (2012).
- [49] A. E. Allahverdyan, K. Hovhannisyan, and G. Mahler, *Optimal refrigerator*, Phys. Rev. E **81**, 051129 (2010).
- [50] Moreover, the instantaneity of the quench and the fact that it does not cause any level crossings ensures that the process is adiabatic also in the sense of the quantum adiabatic theorem.
- [51] Y. Rezek and R. Kosloff, *Irreversible performance of a quantum harmonic heat engine*, New J. Phys. **8**, 83 (2006).
- [52] R. Kosloff and Y. Rezek, *The quantum harmonic Otto cycle*, Entropy **19**, 136 (2017).
- [53] A. Alecce, F. Galve, N. L. Gullo, L. Dell'Anna, F. Plastina, and R. Zambrini, *Quantum otto cycle with inner friction: finite-time and disorder effects*, New J. Phys. **17**, 075007 (2015).
- [54] A. Uhlmann, *The "transition probability" in the state space of a *-algebra*, Rep. Math. Phys. **9**, 273 (1976).
- [55] H. Scutaru, *Fidelity for displaced squeezed thermal states and the oscillator semigroup*, J. Phys. A: Math. Gen. **31**, 3659 (1998).

Appendix A: The effective temperature of the WM during an isochoric interaction

Due to the strong coupling to the bath during the isochoric interaction, the state of the WM will in general acquire non-diagonal terms, leading to the state being, in general, not a thermal state. Indeed, the thermal state is a function of the Hamiltonian and hence cannot have non-diagonal terms in the energy eigenbasis. In this appendix, we introduce a measure of athermality for Gaussian states of an oscillator and show that for the isochoric interactions we consider in the main text (Secs. III and IV) the athermality is insignificant, especially at the end of the interaction. This additionally justifies the view that the thermal bath thermalizes the WM.

Let a single-oscillator Gaussian state be described by a covariance matrix $\sigma_m = \begin{pmatrix} \nu_1 & \kappa \\ \kappa & \nu_2 \end{pmatrix}$. In order to prescribe it a temperature, we symplectic-diagonalize it into its symplectic form $\hat{\sigma}_m = \begin{pmatrix} \nu & 0 \\ 0 & \nu \end{pmatrix}$. Now, if the covariance matrix were of this form, following Eqs. (10) and (11), the temperature would be

$$T_{eff} = \frac{\omega_m}{\ln \frac{\nu+1}{\nu-1}}. \quad (\text{A1})$$

The above temperature is the definition of the effective temperature that we use in Fig. 1. For diagonal covariance matrices, T_{eff} coincides with the real temperature of the system.

In order to define the athermality of the state given by σ_m , $\rho(\sigma_m)$, we compute the Uhlmann fidelity [54] between $\rho(\sigma_m)$ and the thermal state at the effective temperature, $\rho(\hat{\sigma}_m)$, given by

$$F[\sigma_m, \hat{\sigma}_m] = \left(\text{Tr} \sqrt{\sqrt{\rho(\sigma_m)} \rho(\hat{\sigma}_m) \sqrt{\rho(\sigma_m)}} \right)^2. \quad (\text{A2})$$

$F[\sigma_m, \hat{\sigma}_m]$ is equal to 1 if and only if $\sigma_m = \hat{\sigma}_m$, and is < 1 otherwise.

For Gaussian states the Uhlmann fidelity can be directly expressed in terms of their covariance matrices. For purely quadratic states (which recall is the case of thermal states) the fidelity is given by [55]

$$F[\sigma_m, \hat{\sigma}_m] = \frac{2}{\sqrt{A+B} - \sqrt{B}}, \quad (\text{A3})$$

where the quantities A and B are given by

$$A = 4 \det(\sigma_m + \hat{\sigma}_m), \quad (\text{A4})$$

$$B = (4 \det \sigma_m - 1)(4 \det \hat{\sigma}_m - 1). \quad (\text{A5})$$

Now we can look at how much the state of the WM, as given by the covariance matrix $\sigma_m(t)$, differs from the thermal state at temperature T_{eff} —given by the covariance matrix $\hat{\sigma}_m(t)$ —at any moment t during the isochoric interactions described in Secs. III and IV. To that

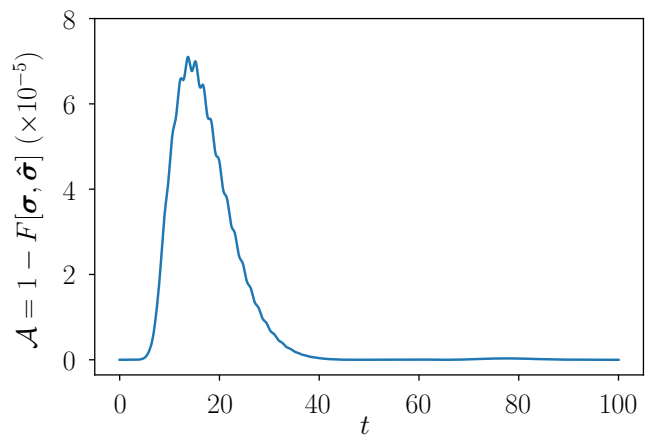


FIG. 7. Time-dependence of the athermality of the WM, initially thermal at temperature $T_b = 0.5$, for the isochoric interaction with a bath (at temperature $T_b = 4$) consisting of $N = 30$ oscillators with frequencies $\omega_b = \omega_m = 2$. The coupling constants are matched so that $\gamma = \alpha = 0.1$ and the interaction lasts $\tau = 100$ units of time, with the ramp-up period δ being 0.1τ . See Sec. III for a detailed explanation of the meaning of these parameters.

end, we define the athermality of the state at a moment t as

$$\mathcal{A}(t) = 1 - F[\sigma_m(t), \hat{\sigma}_m(t)]. \quad (\text{A6})$$

Due to the properties of the fidelity, we thus have that $0 \leq \mathcal{A}(t) \leq 1$ and $\mathcal{A}(t) = 0$ iff $\sigma_m(t) = \hat{\sigma}_m(t)$, i.e., if the state of the system is really thermal.

In Fig. 7 we plot the athermality of the WM for an example isochoric interaction with a bath consisting of $N = 30$ oscillators. We clearly see that, except for a period in the beginning of the process, the WM is rather close to being thermal. It is especially interesting that by the end of the process, the WM is almost exactly thermal. This information, in addition to the final temperature of the WM shown in Fig. 1, indicates that the WM is thermalized by the bath.